J|A|C|S
ARTICLES
Published on Web 02/13/2002

Enantiospecific Desorption of Chiral Compounds from Chiral Cu(643) and Achiral Cu(111) Surfaces

Joshua D. Horvath and Andrew J. Gellman*

Contribution from the Department of Chemical Engineering, Carnegie Mellon University, Pittsburgh, Pennsylvania 15213

Received September 17, 2001

Abstract: Temperature-programmed desorption (TPD) experiments have been conducted to investigate enantiospecific desorption from chiral single-crystal surfaces. The (643) and ($\bar{6}\,\bar{4}\,\bar{3}$) planes of face-centered cubic metals such as Cu have kinked and stepped structures which are nonsuperimposable mirror images of one another and therefore are chiral. These chiral surfaces are denoted Cu(643)^R and Cu(643)^S. We have observed that the desorption energies of (*R*)-3-methylcyclohexanone and (*R*)- and (*S*)-propylene oxides from the Cu(643)^R and Cu(643)^S surfaces depend on the relative handedness of the adsorbate/substrate combination. Since the (643) surface is comprised of terraces with local (111) orientation which are separated by kinked monatomic steps, it is instructive to perform TPD experiments with these chiral compounds on the achiral Cu(111) surface. These experiments have given some insight into the adsorption sites for the chiral molecules on the Cu(643) surfaces. There are several high-temperature features in the TPD spectra of the chiral compounds that only appear in the spectra from the (643) surfaces and thus are attributed to molecules adsorbed at or near the kinked steps. In addition there are lower temperature desorption features observed on the Cu(643) surfaces which occur in the same temperature range as desorption features observed on the Cu(111) surface. These features observed on the (643) surfaces are attributed to desorption from the flat (111) terraces.

1. Introduction

The demand for single-enantiomer chiral compounds in the pharmaceutical industry continues to grow each year.[1] As the demand for single-enantiomer compounds grows, so does the interest in developing new enantioselective processes. A promising route to the development of new enantioselective catalytic or adsorptive processes is the fabrication of novel surfaces with chiral structures. Much recent work on producing chiral surfaces has focused on imparting chirality to achiral surfaces by the irreversible adsorption of chiral molecules onto achiral substrates.[2−4] The resulting chiral surfaces can then be used to perform enantioselective chemical reactions or separations. The work described in this paper focuses on a different class of chiral surfaces, ones which are naturally chiral and are formed by cleaving single crystals of a face-centered cubic (fcc) metal to expose high Miller index surfaces with steps and kinks.

McFadden et al. first pointed out that the (643) and ($\bar{6}\,\bar{4}\,\bar{3}$) surfaces of an fcc crystal are nonsuperimposable mirror images of one another and therefore are chiral.[5] All such surfaces of face-centered cubic crystals having kinked steps are inherently chiral. Figure 1 shows the structure of an fcc (643) surface. The steps are separated by (111) terraces and have kinks at every two lattice spacings. Such surfaces are designated (643)^S and (643)^R, on the basis of the arrangement of the microfacets forming the kinks on the surface. The handedness of these surfaces implies that each should interact differently with one enantiomer of a chiral adsorbate. To determine whether one could observe enantiospecific adsorption of chiral molecules on chiral single-crystal surfaces, McFadden et al. examined the adsorption of (*R*)- and (*S*)-butan-2-ol on Ag(643)^R and Ag(643)^S surfaces.[5] Two types of experiments were conducted to detect enantiospecific interactions between the chiral Ag(643) surfaces and these chiral alcohols. The first experiment measured the desorption energies of (*R*)- and (*S*)-butan-2-ol from the Ag(643)^R and Ag(643)^S surfaces. The second experiment measured the activation barriers to β-hydride elimination for (*R*)- and (*S*)-butane 2-oxide on the Ag(643)^R and Ag(643)^S surfaces. Unfortunately, those experiments did not reveal any enantiospecificity in the interactions of these species with the Ag(643) surfaces. The conclusion was that although the desorption energies or reaction barriers of these molecules must be influenced by the chirality of the Ag(643) surfaces, the enantiospecific energy differences are less than the experimental resolution of $\sim$0.1 kcal/mol.

Theoretical simulations by Sholl et al. have been performed to try to estimate the magnitude that might be expected for enantiospecific interactions of chiral molecules with chiral surfaces and the adsorbate and substrate characteristics that dictate the magnitude of these interactions. These simulations

* To whom correspondence should be addressed.

(1) Stinson, S. C. *Chem. Eng. News* **2000**, *78*, 55.
(2) Lorenzo, M. O.; Baddeley, C. J.; Muryn, C.; Raval, R. *Nature* **2000**, *404*, 376−379.
(3) Blaser, H. U.; Jallet, H. P.; Lottenback, W.; Studer, M. *J. Am. Chem. Soc.* **2000**, *122*, 12675.
(4) Baiker, A. *J. Mol. Catal., A* **1997**, *115*, 473.
(5) McFadden, C. F.; Cremer, P. S.; Gellman, A. J. *Langmuir* **1996**, *12*, 2483−2487.

10.1021/ja012182i CCC: $22.00

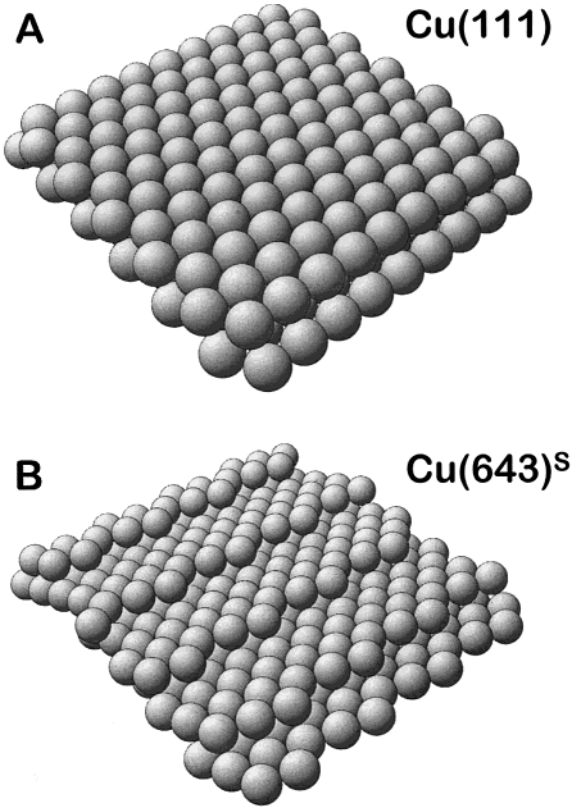

Figure 1. Space-filling models of the (A) Cu(111) and (B) Cu(643)^S surfaces. The (643) surface has a structure formed of kinked steps separated by (111) terraces. The kinked steps give rise to the chirality of the (643) surface. The (111) surface has several planes of mirror symmetry perpendicular to the surface plane and thus is achiral.

have demonstrated that enantiospecific desorption energies can be >1 kcal/mol and should be observable for a number of chiral hydrocarbons on various chiral platinum surfaces.[6−8] The magnitude of the enantiospecific energy differences determined by these simulations is highly dependent on the adsorbate/substrate combination, and there are no obvious trends that can be used to predict the behavior of unexamined systems. Nonetheless, the fact that simulation predicts that such enantiospecific interactions should be observable in some instances has spurred the continued search for such systems.

Electrochemical experiments conducted by Attard et al. provided the first experimental demonstration of the enantiospecific properties of chiral single-crystal surfaces. Enantiospecificity was observed by cyclic voltammetry during the electrooxidation of *d*- and *l*-glucose at Pt(643) and Pt(531) electrodes.[9,10] These investigations compared the cyclic voltammograms of *d*- and *l*-glucose on achiral Pt(111), stepped Pt(211), and stepped Pt(332) surfaces with those on the chiral Pt(643) and Pt(531) surfaces. Similar enantiospecific cyclic voltammetry was observed for the electrooxidation of the chiral sugars mannose, xylose, and arabinose when chiral Pt(321) and Pt(643) electrodes were used.[11] These comparisons clearly revealed that the enantiospecificity of the surfaces could be attributed to the kinked step structures.

Adsorption and desorption are probably the simplest elementary surface processes that one might expect to be enantioselective on a chiral surface, and the theoretical work mentioned above supports this suggestion. As mentioned, electrochemical studies have observed enantioselectivity, however, in a much more complex multistep surface reaction. The objective of the work reported in this paper has been to identify enantioselectivity in an elementary surface process that might then be compared to computational simulation. Recent experimental results have shown that the desorption kinetics of (*R*)-3-methylcyclohexanone and (*R*)- and (*S*)-propylene oxide are influenced by the handedness of the Cu(643) surface.[12,13] The difference in desorption energies between (*R*)-3-methylcyclohexanone on the Cu(643)^R and Cu(643)^S surfaces was measured to be $\Delta\Delta E_{des} = 0.2$ kcal/mol, while (*R*)- and (*S*)-propylene oxides exhibited enantiospecific desorption energy differences of approximately $\Delta\Delta E_{des} = 0.06$ kcal/mol on the chiral Cu(643) surfaces. In this paper we probe the origin of the enantioselectivity in these adsorbate/substrate systems by comparing the desorption characteristics of (*R*)-3-methylcyclohexanone and (*R*)- and (*S*)-propylene oxides from the chiral Cu(643) surfaces with their desorption kinetics from the achiral Cu(111) surface. As mentioned above the (643) surface consists of kinked steps separated by (111) terraces. As expected, desorption experiments conducted using chiral adsorbates on the achiral Cu(111) surface do not show enantiospecific effects. However, the results of the desorption experiments on the Cu(111) surface do provide insight into which sites on the Cu(643) surfaces give rise to enantiospecific features in the desorption spectra from the (643) surfaces.

2. Experimental Section

All experiments were conducted in a stainless steel ultra-high vacuum (UHV) chamber with a base pressure of less than 10^{-10} Torr which has been described in detail elsewhere.[14] The chamber is equipped to perform inert argon ion sputtering, low-energy electron diffraction (LEED), Auger electron spectroscopy (AES), and temperature-programmed desorption (TPD) using a mass spectrometer. The chiral surface was a single-crystal Cu disk 12.5 mm in diameter and 2 mm thick purchased from Monocrystals Co. One side of the sample exposes the (643) surface, and the other side of the sample exposes the $(\bar{6}\,\bar{4}\,\bar{3})$ surface. A second single-crystal Cu disk 10 mm in diameter and 2 mm thick with (111) orientation was purchased from the same vendor. While in the vacuum system, each crystal was spot-welded between two tantalum wires attached to a sample holder at the bottom of a manipulator. Both sides of the (643) crystal were initially cleaned by cycles of 1.0 keV Ar^+ ion bombardment using a current of 10 μA and annealing to 1000 K until no contaminants were detected by AES. Only one side of the (111) crystal was polished, and only the polished side was cleaned and used in this work. Both of the chiral compounds investigated in this paper were found to contaminate the surface with small amounts of carbon after cumulative exposures greater than 1 L (1 L = 10^{-6} Torr·s). To remove carbon contamination after each experiment, the surface was cleaned by Ar^+ ion sputtering and annealing. Typically, the surface was annealed to 1000 K for 60 s every 15 min while the surface was sputtered with 1.0 keV argon ions. In the case of the Cu(643) sample, which has both sides polished, the

(6) Sholl, D. S. *Langmuir* **1998**, *14*, 862−867.
(7) Sholl, D. S.; Asthagiri, A.; Power, T. D. *J. Phys. Chem. B* **2001**, *105*, 4771−4782.
(8) Power, T. D.; Sholl, D. S. *J. Vac. Sci. Technol., A* **1999**, *17*, 1700−1704.
(9) Ahmadi, A.; Attard, G. *Langmuir* **1999**, *15*, 2420−2424.
(10) Attard, G.; Ahmadi, A.; Feliu, J.; Rodes, A.; Herrero, E.; Blais, S.; Jerkiewicz, G. *J. Phys. Chem. B* **1999**, *103*, 1381−1385.
(11) Attard, G. *J. Phys. Chem. B* **2001**, *105*, 3158−3167.
(12) Horvath, J. D.; Gellman, A. J. *J. Am. Chem. Soc.* **2001**, *123*, 7953−7954.
(13) Horvath, J. D.; Gellman, A. J.; Sholl, D. S.; Power, T. D. In *Physical Chemistry of Chirality*; Hicks, J., Ed.; American Chemical Society: Washington, DC, in press.
(14) Gellman, A. J.; Horvath, J. D.; Buelow, M. T. *J. Mol. Catal., A* **2001**, *167*, 3−11.

side of the crystal being sputtered was switched every 15 min, with each side receiving 1 h of sputtering between experiments. Surface cleanliness was verified by AES, and the (643) surface structure was verified by observation of sharp LEED patterns. LEED patterns of these Cu(643)^R and Cu(643)^S surfaces have been described elsewhere.[13,14]

3-Methylcyclohexanone and propylene oxide were each transferred to glass vials and subjected to several cycles of freezing, pumping, and thawing to remove air and other high vapor pressure impurities. The purity of each sample was verified by mass spectrometry. Exposure of the sample surfaces to the adsorbate was performed by introducing the vapor into the UHV chamber through a leak valve while measuring the pressure with the ion gauge. Exposures are reported in langmuirs (L) and are not corrected for ion gauge sensitivity to different gas species.

Temperature-programmed desorption (TPD) experiments were begun by cooling the Cu sample with liquid nitrogen to less than 100 K. The clean Cu surface was then exposed to vapors admitted into the chamber through a leak valve. Desorption measurements were performed by heating the sample at a constant rate while the mass spectrometer monitored the species desorbing from the surface. The mass spectrometer is housed in a stainless steel tube which terminates in a circular aperture approximately 0.75 cm in diameter. Desorption experiments are conducted with the sample approximately 2−3 mm from the end of this aperture, and any desorption from the opposite side of the crystal is undetectable. The result of the TPD experiment is a plot of desorption rate as a function of Cu sample temperature. Using the peak desorption temperatures, T_p, and the heating rate, β, the desorption energies, ΔE_{des}, can be estimated using the relationship developed by Redhead.[15] In principle, adsorbed molecules can either desorb from the surface during heating or decompose to generate gas-phase reaction products. In the systems examined so far, the desorption of chiral molecules was molecular, and thus the TPD experiment can be used to measure desorption kinetics and to estimate desorption energies, ΔE_{des}.

Several control experiments have been performed to verify that the differences observed in the desorption experiments were due to the enantiospecific interactions between the chiral surface and the chiral adsorbate. In the event that only one of the two pure enantiomers of a chiral compound is commercially available, experiments are performed with a racemic mixture of the compound. The racemic mixture is achiral, and should produce the same experimental results on both the right-handed and left-handed surfaces. If both pure enantiomers of a chiral compound are commercially available, experiments are performed using all four possible enantiomer−surface combinations. The combination of a right-handed molecule and a right-handed surface should yield the same experimental results as a left-handed molecule on a left-handed surface. The combination of a right-handed molecule and a left-handed surface should yield the same experimental results as a left-handed molecule on a right-handed surface. Only in cases where both enantiomers of the adsorbate are compared on one surface or cases in which one enantiomer of the adsorbate is studied on both surfaces does one expect to observe enantiospecific effects.

3. Results

3.1. 3-Methylcyclohexanone Desorption from Cu(643) and Cu(111). We have explored the enantiospecific adsorption of 3-methylcyclohexanone on the chiral Cu(643) surfaces and its adsorption on the Cu(111) surface, the plane that forms the terraces of the Cu(643) surfaces. TPD spectra were acquired for (*R*)-3-methylcyclohexanone ((*R*)-3-MCHO) and a racemic mixture of 3-methylcyclohexanone (3-MCHO) on the Cu(643)^R, Cu(643)^S, and Cu(111) surfaces. To prepare for the TPD experiments, the clean surfaces were cooled to 90 K and then exposed to vapor from the background. Figure 2 shows TPD spectra for (*R*)-3-MCHO on the Cu(643)^S surface after exposures in the range 0.05−0.45 L. After the highest exposure, desorption peaks were observed at 385, 346, 222, and 168 K. The peak at 168 K did not saturate with increasing exposure and is due to multilayer desorption. The three higher temperature desorption peaks did not increase further in intensity with increasing exposure to (*R*)-3-MCHO and are due to desorption from the monolayer adsorbed directly on the Cu(643)^S surface. TPD spectra acquired under the same conditions for (*R*)-3-MCHO on Cu(643)^R were qualitatively similar.

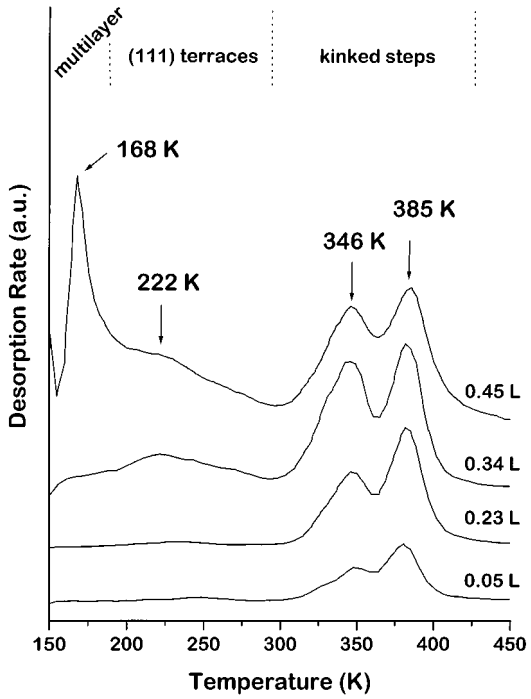

Figure 2. A series of TPD spectra taken following increasing exposures of (*R*)-3-methylcyclohexanone to the Cu(643)^S surface. The two highest temperature peaks (346 and 385 K) correspond to desorption of (*R*)-3-MCHO from the kinked steps on the Cu(643)^S surface. The broad desorption feature at 222 K is associated with desorption from (111) terraces, while the lowest temperature peak (168 K) corresponds to multilayer desorption. Spectra were obtained by heating the surface at 1 K/s while monitoring the ionization fragment at $m/q = 39$. Curves are offset for clarity.

To try to assign the desorption features to specific facets of the Cu(643) structure, we have studied the desorption of (*R*)-3-MCHO from the Cu(111) surface, which has the same structure as the terraces of the Cu(643) surfaces (Figure 1). Figure 3 shows TPD spectra of (*R*)-3-MCHO adsorbed on the Cu(111) surface using background exposures between 0.03 and 0.60 langmuir. At the lowest coverages of (*R*)-3-MCHO there is a single desorption feature at 230 K which grows in intensity with increasing exposures. This feature then saturates in intensity, and a second desorption peak appears at 178 K. The low-temperature peak did not saturate with increasing coverage and arises from multilayer desorption, while the high-temperature peak is due to monolayer desorption. Since the (643) surface has terraces with local (111) orientation, comparing the results of the spectra in Figures 2 and 3 provides some insight into the adsorption sites for (*R*)-3-MCHO on the (643) surface. The ideal (111) surface is perfectly flat with no kinks or steps, although the actual surface used in these experiments is not perfect and is certain to have some defects. Since the peaks at 385 and 346 K appear only in the desorption spectra from the

(15) Redhead, P. A. *Vacuum* **1962**, 203.

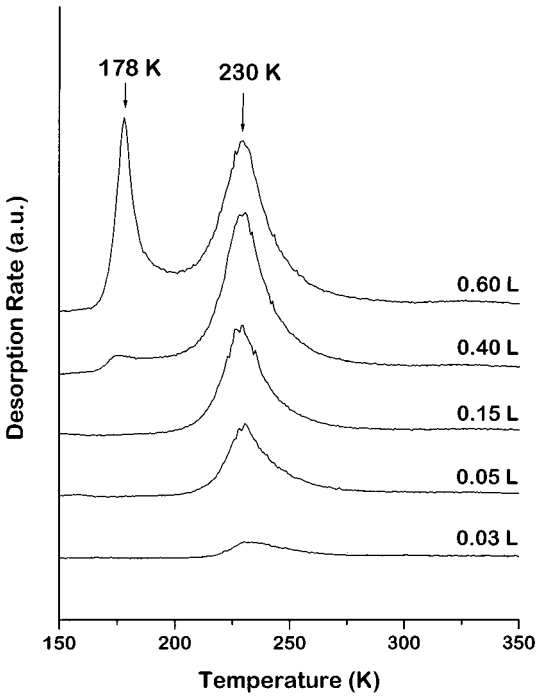

Figure 3. A series of TPD spectra taken following increasing exposures of (*R*)-3-methylcyclohexanone to the Cu(111) surface. The high-temperature peak (~230 K) corresponds to desorption of the (*R*)-3-MCHO monolayer on the Cu(111) surface, while the low-temperature peak (178 K) corresponds to multilayer desorption. Spectra were obtained by heating the surface at 1 K/s while monitoring the ionization fragment at $m/q = 39$. Curves are offset for clarity.

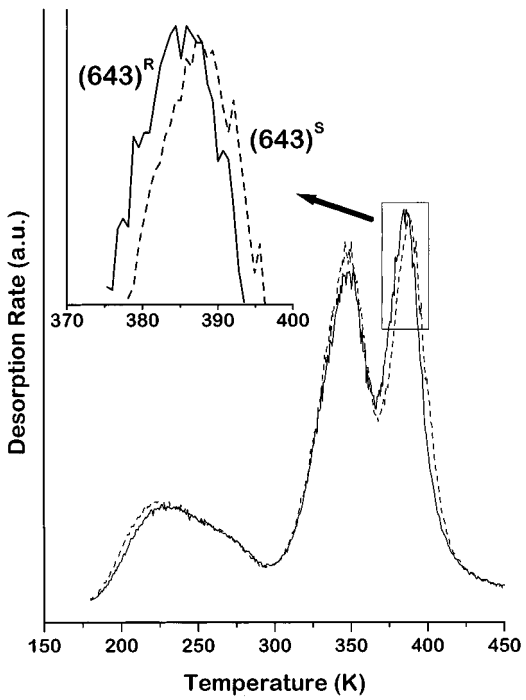

Figure 4. TPD spectra taken following exposures of (*R*)-3-methylcyclohexanone to the Cu(643)^R (solid curve) and Cu(643)^S (dashed curve) surfaces. The inset is a magnified view of the high-temperature peak, which reveals that the desorption peak from the Cu(643)^S surface is shifted by approximately 3.5 K relative to the desorption peak from the Cu(643)^R surface.

stepped and kinked (643) surface and are absent from the desorption spectra obtained from the flat (111) surface, it is likely that these high-temperature desorption features are due to desorption of (*R*)-3-MCHO adsorbed at kinked steps on the (643) surface. Unfortunately, these experiments do not establish the nature of the orientation or the type of interaction of (*R*)-3-MCHO with the kinked step. The TPD spectra also reveal peaks at 222 K on the Cu(643) surface and 230 K on the Cu(111) surface. The fact that this feature appears in spectra from both the flat Cu(111) and the kinked Cu(643) surface suggests that it arises from (*R*)-3-MCHO desorption from the (111) terraces of the Cu(643) surface. In summary, it appears that the desorption features at 346 and 385 K on the chiral Cu(643) surfaces arise from (*R*)-3-MCHO that is adsorbed at the kinked steps, which are the features giving rise to the chirality of these surfaces.

If the Cu(643) surfaces exhibit enantiospecific adsorption of chiral species, this should to be observable by close examination of the desorption temperatures of the high-temperature peaks in the TPD spectra of (*R*)-3-MCHO. TPD experiments were repeated six times for each adsorbate/substrate combination with coverages of one monolayer of 3-MCHO or (*R*)-3-MCHO adsorbed on the surface. Between each experiment the surfaces were cleaned using the sputtering and annealing procedure mentioned in section 2. To determine peak temperatures most accurately, Gaussian curves were fit to each peak using data from a temperature range of ±10 K about each peak. The peak desorption temperatures were determined from the maxima of the fit curves. Using this procedure, peak desorption temperatures for (*R*)-3-MCHO and 3-MCHO on all three surfaces were reproducible with a standard deviation of less than 0.75 K as determined from a set of six nominally identical experiments. Figure 4 shows typical TPD spectra for (*R*)-3-MCHO on both the Cu(643)^R and Cu(643)^S surfaces. Careful examination of the feature at ~385 K reveals a visible difference in the peak desorption temperatures observed for (*R*)-3-MCHO on the Cu(643)^R and Cu(643)^S surfaces. In contrast the desorption features observed at ~222 and ~346 K in the TPD spectra shown in Figure 4 occur at nearly identical temperatures. Figure 5 shows the average peak desorption temperatures for (*R*)-3-MCHO and 3-MCHO desorption from the Cu(643)^R, Cu(643)^S, and Cu(111) surfaces. The peak at ~385 K on the Cu(643) surfaces does not reveal enantioselective desorption of the racemic 3-MCHO. The average peak desorption temperatures for racemic 3-MCHO on the Cu(643)^R and Cu(643)^S surfaces are nearly identical. Of course, this is a control experiment and should not reveal any enantiospecificity since the racemic mixture has no net chirality. The experiment does, however, reveal the accuracy with which we have been able to reproduce the peak desorption temperatures. As a second possible control experiment we have compared the desorption of pure component (*R*)-3-MCHO and racemic 3-MCHO from the achiral Cu(111) surface. Figure 5 reveals that once again there is no significant difference in the peak desorption temperatures of these two adsorbates. It should be noted, however, that this need not be the case. Although the Cu(111) surface is achiral and thus should not interact enantiospecifically with either pure (*R*)-3-MCHO or (*S*)-3-MCHO, it is not necessarily the case that the adsorbed racemic mixture should have the same characteristics as the pure enantiomers. This statement is equivalent to the fact that while the melting and boiling points of pure enantiomers are identical they are quite often different from the melting and boiling points of the racemic mixture. The fact that the racemic mixture of

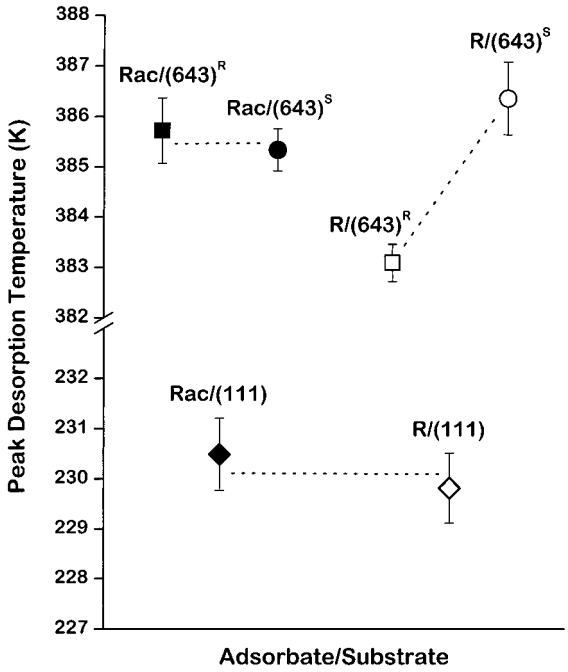

Figure 5. Average peak desorption temperatures of (*R*)-3-methylcyclohexanone (R) and racemic 3-methylcyclohexanone (Rac) on the Cu(643)^R, Cu(643)^S, and Cu(111) surfaces. The error bars correspond to one standard deviation in the temperature measurement and have been determined from six repetitions of each TPD spectrum. The differences in the desorption temperatures of (*R*)-3-MCHO from the Cu(643) surfaces reveal significant enantiospecificity.

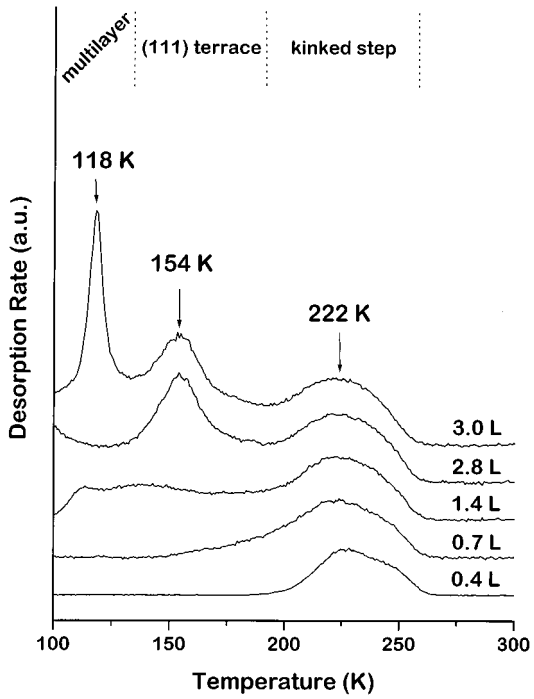

Figure 6. A series of TPD spectra taken following increasing exposures of (*R*)-propylene oxide to the Cu(643)^R surface. The highest temperature peak (~222 K) is associated with desorption of (*R*)-propylene oxide from the kinked steps, while the peak at ~154 K is associated with desorption from the (111) terraces of the Cu(643)^R surface. The lowest temperature peak (118 K) corresponds to multilayer desorption. Spectra were obtained by heating the surface at 1 K/s while monitoring the ionization fragment at $m/q = 27$. Curves are offset for clarity.

3-MCHO and the pure component (*R*)-3-MCHO have the same desorption kinetics when adsorbed on the Cu(111) surface suggests that the adsorbed racemic mixture may separate into domains of pure (*R*)-3-MCHO or (*S*)-3-MCHO.

The key result of our study of the desorption of (*R*)-3-MCHO comes from the comparison of the peak desorption temperatures of (*R*)-3-MCHO on the Cu(643)^R and Cu(643)^S surfaces. The average peak desorption temperature for (*R*)-3-MCHO on the Cu(643)^R surface is 3.5 K lower than the average peak desorption temperature on the Cu(643)^S surface. The difference in the peak desorption temperatures is $\Delta T_p = 3.5 \pm 0.8$ K and thus is statistically significant. These results clearly reveal enantiospecificity in the desorption kinetics of the enantiomerically pure (*R*)-3-MCHO on the chiral Cu(643) surfaces. The observation of enantioselectivity in the desorption of (*R*)-3-MCHO on the chiral Cu(643) surfaces has relied on study of the high-temperature feature ($T_p \approx 385$ K) in the TPD spectra. The peak at 346 K is also associated with desorption from the kinked steps and has been analyzed. Unfortunately, this peak is somewhat broader than the peak at 385 K, and the peak desorption temperature is more sensitive to experimental conditions. No enantiospecificity was observed in the desorption feature at 346 K.

3.2. (*R*)- and (*S*)-Propylene Oxide Desorption from Cu(643) and Cu(111). The desorption of propylene oxides from the Cu(643) surface has been studied to try to observe enantiospecificity. The advantage of this adsorbate over 3-methylcyclohexanone is that both pure enantiomers of propylene oxide are available commercially and thus this system offers an opportunity to observe a true diastereomeric effect in the desorption of chiral adsorbates from chiral substrates. TPD spectra were acquired for both (*R*)- and (*S*)-propylene oxide on the Cu(643) and Cu(111) surfaces. Figure 6 shows TPD spectra following increasing exposures of (*R*)-propylene oxide to the Cu(643)^R surface. The surfaces were prepared using background exposures to (*R*)-propylene oxide ranging from 0.4 to 3.0 langmuirs with the surface at 90 K. Three peaks are visible in the desorption spectrum obtained after the highest exposure. The lowest temperature peak at 118 K did not saturate with increasing exposure and arises from multilayer desorption. The peaks at 154 and 222 K saturated in intensity with increasing exposure and are believed to arise from desorption of the (*R*)-propylene oxide monolayer interacting directly with the Cu(643)^R surface. TPD spectra obtained for (*R*)-propylene oxide on the Cu(643)^S surface and for (*S*)-propylene oxide on the Cu(643)^R and Cu(643)^S surfaces were qualitatively similar to those shown in Figure 6.

To try to assess the origins of the desorption features on the Cu(643) surfaces, we have studied the desorption of the propylene oxides from the Cu(111) surface. Figure 7 shows TPD spectra obtained following increasing exposures of (*R*)-propylene oxide to the achiral Cu(111) surface. Only two peaks are visible in the desorption spectrum. The peak at 121 K arises from multilayer desorption, while the feature at 145 K arises from monolayer desorption. Comparison of the spectra in Figures 6 and 7 reveals some interesting similarities. The multilayer desorption temperatures observed for (*R*)-propylene oxide on the Cu(643)^R and Cu(111) surfaces are nearly identical. The features observed at 154 K on the Cu(643)^R surface and 145 K on the Cu(111) surface have approximately the same desorption temperatures and similar shapes in both sets of spectra. This comparison suggests that the feature observed at 154 K during

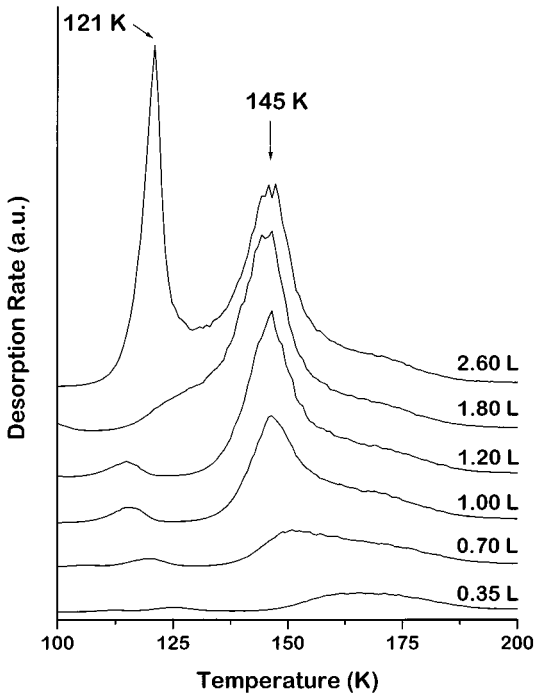

Figure 7. A series of TPD spectra taken following increasing exposures of (*R*)-propylene oxide to the Cu(111) surface. The high-temperature peak (145 K) corresponds to monolayer desorption from the Cu(111) surface, while the low-temperature peak (121 K) corresponds to multilayer desorption. Spectra were obtained by heating the surface at 1 K/s while monitoring the ionization fragment at $m/q = 27$. Curves are offset for clarity.

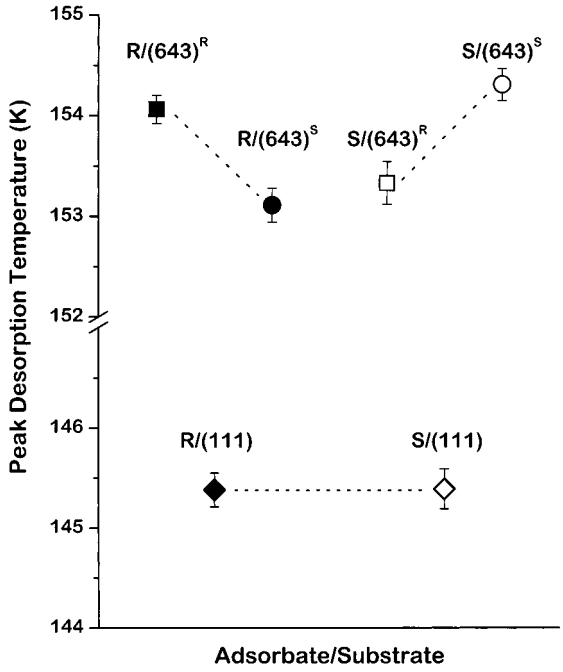

Figure 8. Average peak desorption temperatures of (*R*)- and (*S*)-propylene oxides on the Cu(643)^R, Cu(643)^S, and Cu(111) surfaces. Error bars correspond to one standard deviation in the temperature measurements and have been determined from six repetitions of each TPD spectrum. The results on the Cu(643) surfaces reveal a clear and significant diastereomeric effect.

desorption from the Cu(643) surface is due to (*R*)-propylene oxide desorption from the flat (111) terraces of the Cu(643) surface. In contrast, the peak at 222 K appears only in the TPD spectra obtained from the stepped and kinked Cu(643) surface and is absent from TPD spectra obtained from the flat Cu(111) surface. This suggests that the desorption feature at 222 K on the Cu(643) surface is due to (*R*)-propylene oxide adsorbed at the kinked steps of the Cu(643) surface.

To observe a diastereomeric effect in the desorption kinetics of propylene oxide from a chiral surface, both enantiomers have been adsorbed and desorbed from both enantiomers of the chiral Cu(643) surface. TPD experiments were repeated six times for each adsorbate/substrate combination with coverages of one monolayer of (*R*)- or (*S*)-propylene oxide adsorbed on the surface. Prior to each TPD experiment the surface was cleaned and annealed. Coverages of one monolayer were achieved by exposing the Cu surface to propylene oxide while holding the surface at a temperature that was a few degrees above the multilayer desorption temperature. Peak desorption temperatures were determined by fitting Gaussian curves to the data over a temperature range of ± 12.5 K about the 154 K peak and ± 20 K about the 222 K peak. Using this analysis, the peak at 222 K on the Cu(643) surface did not reveal significant enantiospecificity, probably because its width gave rise to large standard deviations in the peak temperature measurement. Analysis of the desorption feature at $\sim$154 K, however, does reveal a significant diastereomeric effect. At first this may seem a little surprising since we have already associated this feature with desorption from the achiral (111) terraces. It is possible, however, that the effects of the chirality of the kinked step can be transmitted to molecules on the (111) terraces through interactions with molecules adsorbed at the kinked step. This chiral transmission mechanism will be discussed in section 4.2. The desorption peak at 154 K is significantly narrower than the peak at 222 K, and we have been able to measure the peak desorption temperature to an accuracy of better than ± 0.2 K. Figure 8 shows the average peak desorption temperatures for (*R*)- and (*S*)-propylene oxide on the Cu(643)^R, Cu(643)^S, and Cu(111) surfaces. Figure 8 reveals enantiospecific desorption kinetics for the enantiomerically pure compounds on the chiral Cu(643) surfaces. The peak desorption temperatures for (*R*)-propylene oxide are about 1 K higher on the Cu(643)^R surface than on the Cu(643)^S surface. Similarly, peak desorption temperatures for (*S*)-propylene oxide are about 1 K lower on the Cu(643)^R surface than on the Cu(643)^S surface. The expected diastereomeric effect for this adsorbate/substrate system is clearly revealed. The difference in the peak desorption temperatures is $\Delta T_p = 1.0 \pm 0.3$ K and is statistically significant. Several control experiments have been performed to check this result. The peak desorption temperature for (*R*)-propylene oxide on Cu(643)^R is nearly identical to that of (*S*)-propylene oxide on Cu(643)^S. Similarly, the peak desorption temperatures for (*R*)-propylene oxide on Cu(643)^S and (*S*)-propylene oxide on Cu(643)^R are not significantly different. As a final check, TPD experiments were conducted with (*R*)- and (*S*)-propylene oxides on the achiral Cu(111) surface. Figure 8 indicates that the peak desorption temperatures for (*R*)- and (*S*)-propylene oxides on the achiral Cu(111) surface are nearly identical, as expected for desorption from an achiral surface. This control experiment verifies the reproducibility of the data obtained with these methods and is further evidence that the desorption of chiral compounds from the Cu(643) surfaces is influenced by the chirality of the surface.

4. Discussion

The desorption of several simple chiral molecules from the chiral Cu(643) and achiral Cu(111) surfaces has been explored using TPD. (*R*)-3-MCHO and (*R*)- and (*S*)-propylene oxides exhibit enantiospecificity in the temperatures at which they desorb from the Cu(643)^R and Cu(643)^S surfaces. Control experiments performed on the achiral Cu(111) surface have verified that the enantiospecific desorption properties observed on the Cu(643) surfaces are indeed due to surface chirality.

It should be noted that although enantiospecific desorption has been observed for (*R*)-3-methylcyclohexanone and (*R*)- and (*S*)-propylene oxides on the Cu(643) surfaces, several other chiral adsorbates did not exhibit any enantiospecific desorption characteristics that could be observed with the experimental resolution available. A saturated monolayer of (*S*)-limonene has a peak desorption temperature of 350.6 ± 0.2 K on the Cu(643)^R surface, and a peak desorption temperature of 350.5 ± 0.2 K on the Cu(643)^S surface. Similar results are observed for (*R*)-limonene on the same surfaces. The fact that a chiral adsorbate does not exhibit enantiospecific desorption from a chiral surface is not completely surprising since theoretical simulations of chiral hydrocarbon adsorption on chiral Pt surfaces by Sholl et al. predict that some adsorbate/substrate combinations will exhibit practically no enantiospecificity, while other adsorbate/substrate combinations do show enantiospecific desorption energy differences that should be detectable using TPD.[7] Ultimately, it is hoped that the criteria that determine the magnitude of enantiospecific desorption energetics should become apparent and begin to guide future experiments; however, the body of experimental and simulation data in hand is not yet sufficient to provide this level of insight.

It is worth noting that the enantiospecific effects observed in these experiments are found by examining an elementary reaction step, the molecular desorption of a molecule from a metal surface. Other examples of enantiospecific chemistry on naturally chiral surfaces have been observed for the electrooxidation of *d*- and *l*-glucose and other molecules at chiral Pt electrodes.[9−11] However, these electrochemical experiments involve far more complicated chemistry as the glucose molecules decompose on the chiral Pt surface during the electrooxidation process. Sholl et al. have been successful in simulating the adsorption of chiral hydrocarbons on chiral Pt surfaces for simple hydrocarbons that do not decompose on the surface.[6−8] Simulation of the molecular desorption of a molecule from a metal surface should be easier than the simulation of processes involving multistep decomposition reactions. Thus, the desorption experiments described in this work bring us closer to establishing a connection with the results of computational simulation.

4.1. Enantiospecific Desorption Energetics. The TPD experiments can be used to estimate the desorption energies, ΔE_{des}, of adsorbates on surfaces. The enantiospecificity observed in the desorption kinetics of (*R*)-3-methylcyclohexanone and (*R*)- and (*S*)-propylene oxides on the Cu(643) surfaces arises from enantiospecific differences in desorption energies, $\Delta\Delta E_{des}$. The TPD experiments then estimate the $\Delta\Delta E_{des}$ between two enantiomers on the same chiral surface or equivalently the $\Delta\Delta E_{des}$ for one enantiomer adsorbed on the two enantiomers of a chiral surface. The ΔE_{des} values were calculated using the Redhead relation[15] for first-order desorption kinetics using the average peak desorption temperatures, T_p, obtained from the TPD experiments:

$$\frac{\Delta E_{des}}{RT_p^{\,2}} = \frac{\nu}{\beta}\exp\left(\frac{-\Delta E_{des}}{RT_p}\right)$$

Table 1. T_p and ΔE_{des} for Several Chiral Adsorbate/Substrate Pairs

system	av T_p (K)	av ΔE_{des} (kcal/mol)
(*R*)-3-MCHO/Cu(643)^R	383.1 ± 0.4	24.65 ± 0.03
(*R*)-3-MCHO/Cu(643)^S	386.4 ± 0.7	24.88 ± 0.05
(*R*)-propylene oxide/Cu(643)^R	154.1 ± 0.2	9.65 ± 0.01
(*R*)-propylene oxide/Cu(643)^S	153.1 ± 0.2	9.58 ± 0.01
(*S*)-propylene oxide/Cu(643)^R	153.3 ± 0.2	9.59 ± 0.01
(*S*)-propylene oxide/Cu(643)^S	154.3 ± 0.2	9.66 ± 0.01

The ΔE_{des} and T_p for each adsorbate/substrate combination are summarized in Table 1. The preexponential factor, ν, for each chiral adsorbate was assumed to be 10^{13} s^{-1}. In principle, the preexponents, ν, can be enantiospecific; however, we have not tried to measure this. Even if there is some error in the assumed preexponential factor, the relative differences in desorption energies, $\Delta\Delta E_{des}$, between different enantiomer/substrate combinations are relevant. For (*R*)-3-MCHO on the Cu(643)^R and Cu(643)^S surfaces $\Delta\Delta E_{des} \approx 0.2$ kcal/mol and corresponds to a difference of roughly 30% in desorption rates at room temperature. The enantiospecific desorption energy difference for propylene oxide desorption from the Cu(643) surfaces is $\Delta\Delta E_{des} \approx 0.06$ kcal/mol. This corresponds to a 10% difference in the desorption rates of the propylene oxide enantiomers on the Cu(643)^R and Cu(643)^S surfaces at room temperature. Despite the small differences in desorption rates, they are potentially useful from a practical perspective since enantioselective processes can be designed to exploit small differences in physical properties. For example, chromatographic separations that involve multiple adsorption−desorption steps can amplify these differences in desorption rates by many orders of magnitude.

4.2. Chiral Adsorption Sites on the Cu(643) Surface. Some words should be said about the nature of the adsorption sites for the chiral molecules on the Cu(643) surfaces. Since the Cu(643) surfaces have terraces with (111) orientation, comparing TPD spectra from the Cu(643) and Cu(111) surfaces provides some insight into the adsorption sites for chiral molecules on the Cu(643) surfaces. For both (*R*)-3-MCHO and (*R*)- and (*S*)-propylene oxides, the highest temperature desorption features for the (643) surfaces are absent from the TPD spectra obtained from the (111) surfaces. Furthermore, for both molecules there are low-temperature features in the TPD spectra from the Cu(643) surfaces that correspond to those observed from the Cu(111) surfaces. These results strongly suggest that the highest temperature desorption features in the spectra from the Cu(643) surfaces result from desorption of molecules adsorbed at the kinks or steps. The low-temperature features are presumed to arise from desorption from the (111) terraces.

In the case of the propylene oxides on the Cu(643) surfaces, the desorption peak at 222 K in Figure 6 is associated with desorption from the kinked steps while the peak at 154 K is associated with desorption from the (111) terraces. One question is whether the structure of the Cu(643) surface shown in Figure 1 has sufficient area per unit cell to accommodate adsorption

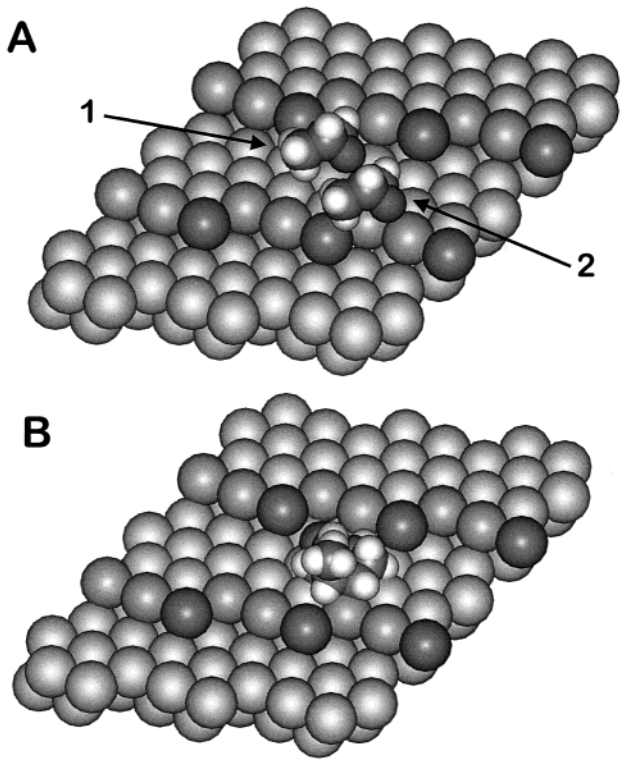

Figure 9. (A) Space-filling model of two (*R*)-propylene oxide molecules adsorbed on the Cu(643)^R surface. The step edges of the surface are shaded darker than the terraces for clarity. The orientation of the propylene oxide is shown with the methyl groups to the left and the oxygen atom of the COC ring to the right from the viewer's perspective. Molecule 1 is adsorbed next to the step edge, while molecule 2 is adsorbed on the terrace away from the step edge. (B) Space-filling model of one (*R*)-3-methylcyclohexanone molecule adsorbed on the Cu(643)^R surface. The orientation of the (*R*)-3-methylcyclohexanone is shown with the ring plane parallel to the surface, the methyl group pointing toward the viewer, and the carbonyl oxygen atom pointing back toward the kink. These orientations have been chosen arbitrarily and are *not* the result of any computational structure determination. The point of this figure is to demonstrate that the (643) terraces are wider than the adsorbed molecules. In the case of the propylene oxide one can imagine two molecules fitting into the surface unit cell.

of propylene oxide both at the step edge and on the terrace. Before this issue is addressed though, it is appropriate to discuss the relationship between the structure shown for the Cu(643) surface and what is probably the true, relaxed structure of these crystal surfaces. LEED patterns have shown that the perfect crystalline array of Figure 1 is a good representation of the average structure of the Cu(643) crystal surfaces used in this work.[13,14] However, in reality the structure of the surface is likely to be imperfect. Imperfections in the surface and the simple thermal equilibration of steps and kinks will create a surface on which there is a distribution of terrace widths and a distribution of step lengths between kinks. These effects have been simulated for chiral Pt surfaces, and it has been shown that they result in a net reduction in the number of kinks on the surface but no significant reduction in the net handedness of the surface.[7] In other words, there is some coalescence of kinks but no significant generation of kinks that are of handedness opposite that of the kinks on the perfect, unrelaxed surface. With these thoughts and caveats in mind one can look at models of propylene oxide adsorption on the perfect Cu(643) surface as shown in Figure 9. This depicts space-filling models for the adsorption of two (*R*)-propylene oxide molecules on the Cu(643)^R surface. The orientations of the molecules have been chosen arbitrarily since we have no knowledge of their structures and the point of the figure is merely to give some idea of the relative sizes of propylene oxide and the unit cell on the Cu(643) surface. One molecule is adsorbed near the step edge, while the other is adsorbed on the terrace, away from the step edge. The first thing to note is that there appears to be "room" for the adsorption of two molecules per unit cell. Since adsorption sites at the kink or step edge allow an adsorbed molecule to interact with more Cu atoms than adsorption on the flat terrace, the ΔE_{des} and desorption temperatures of molecules adsorbed at a kink or step edge should be higher than those of molecules adsorbed on the terrace. This is consistent with the TPD spectra of propylene oxide on the Cu(643) and the Cu(111) surfaces shown in Figures 6 and 7. The final point of note concerning the enantiospecific desorption of the propylene oxide from the Cu(643) surface is that the enantiospecificity that we report arises in the peak with $T_p = 154$ K that we suggest arises from desorption from the (111) terraces. At first glance one might expect that enantiospecificity should be observed in the kinetics of desorption from the kinked steps rather than the terraces. While enantiospecific desorption from the kinked steps probably does occur, the width of the desorption features from the kinked steps (at 222 K in Figure 6) has precluded measurement of the T_p with sufficient accuracy to allow us to observe the enantiospecificity. The fact that we observe enantiospecificity in the desorption from the (111) terraces of the Cu(643) structure is quite interesting. Examination of Figure 9 suggests that this can occur through two mechanisms. On one hand, the propylene oxide on the terrace is adjacent to a molecule adsorbed at a chiral step edge and thus feels a chiral environment that is transmitted across the surface by the molecules at the step edge. Alternatively, the molecules on the terrace are forced to sit adjacent to the top edge of a kinked step that is also chiral and thus creates a chiral adsorption environment. Either of these mechanisms could account for the enantiospecificity observed in the desorption of propylene oxide from the (111) terraces of the Cu(643) surface.

The TPD spectra can also be used to understand something about the nature of the chiral adsorption sites for (*R*)-3-MCHO on the Cu(643) and Cu(111) surfaces. The peaks at 346 K and 385 K in the spectra of Figure 2 are associated with desorption from the kinked steps, while the broad feature at 222 K is associated with desorption from the (111) terraces. Figure 9 shows a space-filling model of (*R*)-3-MCHO adsorbed on the Cu(643) surface. As in the model of propylene oxide, the orientation of the (*R*)-3-MCHO molecule has been chosen arbitrarily since we have no knowledge of its structure and the point of the figure is merely to give some idea of the relative sizes of the (*R*)-3-MCHO and the unit cell on the Cu(643) surface. (*R*)-3-MCHO is much larger than propylene oxide, and it does not appear that there is room on the surface for adsorption of a second molecule on the terrace of the ideal unit cell. The probable origin of the desorption that appears to arise from terraces is regions of the surface in which the terraces are wider than the three-atom-wide terraces of the ideal Cu(643) surface. The reason for the appearance of two high-temperature desorption features is not clear at this point. In contrast with the case of the propylene oxides it is the desorption of (*R*)-3-MCHO from the kinked steps that exhibits the enantiospecific desorption kinetics.

5. Conclusions

The desorption of both (*R*)- and (*S*)-propylene oxide and the desorption of (*R*)-3-methylcyclohexanone from the chiral Cu(643) surface exhibit enantiospecific desorption kinetics. In the case of the propylene oxide, the enantiospecificity is exhibited in the desorption from the terraces of the Cu(643) surface while (*R*)-3-methylcyclohexanone exhibits enantiospecific desorption from the kinked steps of the Cu(643) surface. The enantiospecificity arises from enantiospecific differences in the desorption energies. These results represent the first experimental observations of such enantiospecific desorption kinetics on the naturally chiral surfaces.

Acknowledgment. This work was supported by NSF Grant CTS-9813937.

JA012182I